2.1 *Nuclear Physics* **A251** (1975) 479–492; © *North-Holland Publishing Co., Amsterdam*

TOTAL NUCLEAR PHOTON ABSORPTION CROSS SECTIONS FOR SOME LIGHT ELEMENTS

J. AHRENS, H. BORCHERT†, K. H. CZOCK††, H. B. EPPLER, H. GIMM, H. GUNDRUM†††, M. KRÖNING, P. RIEHN, G. SITA RAM‡, A. ZIEGER and B. ZIEGLER

Max-Planck-Institute for Chemistry, Nuclear Physics Division, Mainz, Germany

Received 23 October 1974
(Revised 7 March 1975)

Abstract: Absolute nuclear photon absorption cross sections have been measured for the elements Li, Be, C, O, Al, Si and Ca from 10 MeV up to photon energies beyond the meson production threshold. Magnetic Compton spectrometers and a bremsstrahlung spectrum with fixed end-point energy were used. The cross sections show structure in the region of the giant resonance and fall off smoothly towards higher energies. In the giant resonance region recent 1p-1h calculations are in poor agreement with these measurements except for one calculation for carbon, which included low lying excited states of the residual mass-11 system. The cross section in the intermediate region (40 to 140 MeV) can be described by the quasideuteron model with the density of deuteron-like structures taken as $8\ NZ/A$. The moments of the measured cross sections are compared with sum rule predictions. The integrated cross sections from 10 MeV up to the meson production threshold (140 MeV) exceed the classical dipole sum by a factor of 1.4 to 2.

E NUCLEAR REACTIONS Li, Be, C, O, Al, Si, Ca(γ, X), E = 10 MeV to above meson threshold; measured total $\sigma(E)$. Natural targets.

1. Introduction

The total cross section $\sigma_{\gamma,T}(E)$ for the nuclear absorption of photons of energy E, can be used to test the validity, not only of nuclear model calculations, but also of model independent theoretical predictions (sum rules) concerning the nucleus [1]). From considerations of fundamental properties of nuclei, these sum rules predict values for some moments of $\sigma_{\gamma,T}(E)$. To test these predictions, a knowledge of cross sections between the particle emission and meson production thresholds is needed. The difficulties inherent in measuring $\sigma_{\gamma,T}(E)$, either directly, or by measuring the partial cross sections [e.g. (γ, n), (γ, p), etc.], have, however, in the past not resulted in data with sufficient accuracy and energy range to seriously test the sum rule predictions.

In this paper the results of measurements of the total nuclear photon absorption cross section for the elements Li, Be, C, O, Al, Si and Ca are presented in the energy

† Now at Institut für Reaktorsicherheit, TÜV Cologne.
†† At present at the IAEA, Vienna.
††† Now at JENAer Glaswerk Schott & Gen., Mainz.
‡ At presen at University of Dar-es-Salaam, Tanzania.

range 10 MeV to energies beyond the meson production threshold (160 MeV at least).

In principle, this measurement of $\sigma_{\gamma,T}(E)$ is similar to earlier experiments[2]), but in the present measurement a more intense bremsstrahlung beam, higher bremsstrahlung end-point energy and better spectrometer resolution result in more accurate measurements over a wider energy range. Details of the Compton spectrometers and the general measuring procedure used in this experiment have been presented elsewhere [3]).

In sect. 2 a short outline of the experimental procedure is given and in sect. 3 an extensive discussion of the error sources is presented. Sect. 4 presents the measured total nuclear photon absorption cross sections in the form of cross section curves and of tables of moments and mean energies. In sect. 5 these cross sections are discussed and compared with theoretical results.

2. Experimental procedure

The results given in this paper have been obtained in a narrow beam photon attenuation experiment, in which thick targets of the materials under investigation were used as absorbers. The total attenuation cross section $\sigma_{tot}(E)$ as a function of the

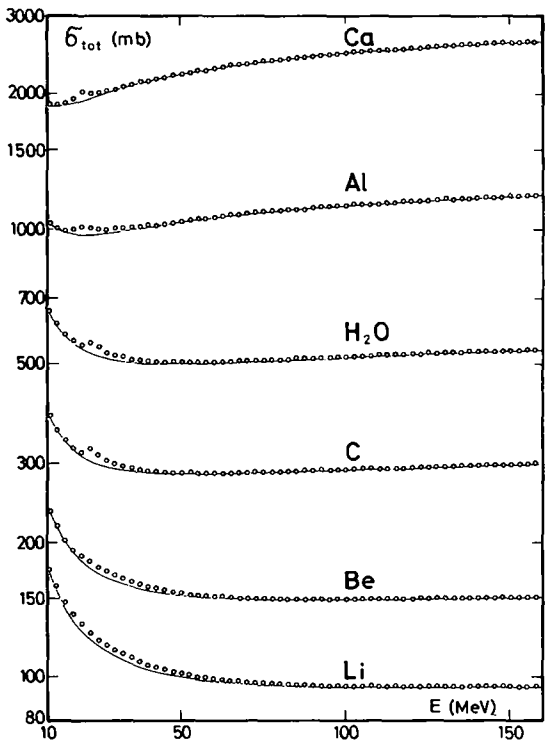

Fig. 1. Measured total attenuation cross sections σ_{tot}. The error bars are smaller than the symbols. The solid lines give the calculated non-nuclear cross sections.

photon energy E can be deduced from the absorption law

$$N(E) = N_0(E) \exp(-n\sigma_{tot}(E)),$$

where N_0 and N are the numbers of photons in a certain energy bin without and with attenuation, respectively, and n is the number of nuclei per cm^2 in the absorber.

In order to obtain the total nuclear photon absorption cross section $\sigma_{\gamma,T}(E)$, the non-nuclear (electronic) cross section $\sigma_{el}(E)$ has to be subtracted from the measured total attenuation cross section $\sigma_{tot}(E)$. The non-nuclear cross section $\sigma_{el}(E)$ was calculated. A brief description of the factors involved in this computation is given in sect. 3.

The experiment was performed using a bremsstrahlung beam produced by electrons from the Mainz linear accelerator [4]). The electron beam was pulsed at a rate of 150 s^{-1} and had a pulse length of 3μs. In the well collimated bremsstrahlung beam an average photon flux of 10^9 photons/MeV · s was obtained at 20 MeV photon energy. The end energy of the bremsstrahlung spectrum was fixed at 140, 200 and 275 MeV for the measurements below 100 MeV, between 100 MeV and 140 MeV and above 140 MeV, respectively.

TABLE 1

Attenuator characteristics and systematic errors

Element	Density ρ (g · cm^{-3})	Length x (cm)	Diameter (cm)	Weight (g)	$\Delta(\rho x)/(\rho x)$ (%)	Impurities (%)	Condition	$\Delta\sigma_{\gamma,T}$ dead time (mb)
Li	0.53618	200.1	1.983 ± 0.002	331.40 ± 0.15	0.25	0.024	metal	0.08
Be	1.843	120.72	2.029 ± 0.001	718.34 ± 0.03	0.1	0.448	metal	0.06
C	1.7653 1.7670 1.7666 2.0694	60.135 80.178 100.22 71.955			0.2	0.001	graphite	0.13
O	0.9982 ± 0.0002	119.50 ± 0.05			0.06	0.001	water	0.2
Al	2.6981 ± 0.0001	42.008 ± 0.004			0.013	0.001	metal	0.34
Si	2.3290 ± 0.0001	41.264 ± 0.004			0.014	0.001	metal mono-crystallin	0.43
Ca	1.5215	49.99	3.389 ± 0.001 4.915 ± 0.001	342.78 ± 0.03 722.02 ± 0.03	0.054	0.016	metal	0.81

The number of nuclei per cm^2 can either be calculated by means of the density ρ, and length x, or by means of the diameter and weight of the absorbers. The systematic error in the number of nuclei per cm^2 is given as $\Delta(\rho x)/(\rho x)$. "$\Delta\sigma_{\gamma,T}$ dead time" is the systematic error resulting from uncertainties in the dead time correction.

The experimental set-up [3]) consisted of two identical 11-channel magnetic Compton spectrometers in the photon beam. These spectrometers had a resolution of approximately 1 % (FWHM) over the entire energy region of the measurement. The absorption target could be inserted into the beam between the spectrometers. The downstream spectrometer was used as the main γ-spectrometer whilst the upstream spectrometer was used for normalization.

The ratio of the photon numbers $N_0(E)$ and $N(E)$ was obtained by measuring the number of Compton electrons from the target of the main spectrometer without and with the absorber in the beam. The number of Compton electrons was determined by subtracting the number of pair positons, which was measured separately with reversed magnetic fields, from the measured number of negatons.

During data taking, a Honeywell DDP 516 computer was used for on-line analysis, and regular checks of the experimental apparatus were made. One hour of beam time yielded eleven cross section values, each with a statistical error of 0.5 %. The total amount of beam time needed to measure the absorption cross section of one absorption target was three to four weeks.

The total absorption cross sections of Li, Be, C, H_2O, Al and Ca are given in fig. 1. The attenuator properties are listed in table 1. All samples were of natural isotopic composition.

3. Data analysis and discussion of errors

In the on-line data analysis, the measured numbers of negatons and positons were corrected for dead time losses [3]) and for counter to counter scattering, which is different for positons and negatons. The positon numbers were corrected for annihilation losses in the target and in the counters. The latter two corrections have not been applied to the preliminary data reported in ref. [5]).

The sum of all non-nuclear cross sections $\sigma_{cl}(E)$ (mainly Compton cross section and cross sections for electron pair production) had to be subtracted from the measured total absorption cross section $\sigma_{tot}(E)$ in order to obtain the total nuclear absorption cross section $\sigma_{\gamma,T}(E)$. The error in $\sigma_{\gamma,T}(E)$ contains contributions from different sources which will now be considered.

(a) The errors due to counting statistics for the two Compton spectrometers have been treated separately since they influence the errors of the final cross sections in different ways. The statistics of each individual counter of the main spectrometer behind the absorber position enter directly into the error of each of the eleven individual cross section values obtained at one energy setting of the spectrometers, whilst the counting statistics of the normalizing spectrometer in front of the absorber position has equal influence on all eleven cross section values. Both contributions to the statistical errors are displayed separately in figs. 2 to 8, where the lengths of the error bars given to the cross section points are determined by the counting statistics of the main spectrometer and the dashed lines along the abscissa indicate the magnitude of possible oscillations produced by the statistics of the normalizing

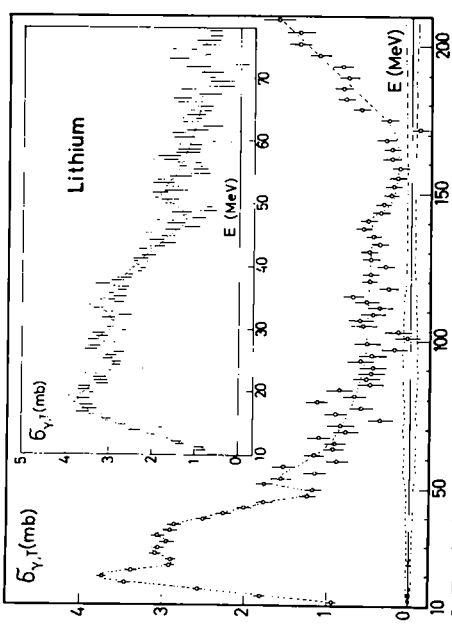

Fig. 2. Total photonuclear cross section for natural Li. The error bars indicate one standard deviation of counting statistics from the main spectrometer. The dashed lines along the abscissa indicate the uncertainty due to counting statistics in the normalizing spectrometer. Oscillations of the base line within this area are possible, the period of these oscillations, however, must not be smaller than 10% in photon energy. The dashed and dotted lines through the cross section values have been drawn to guide the eye.

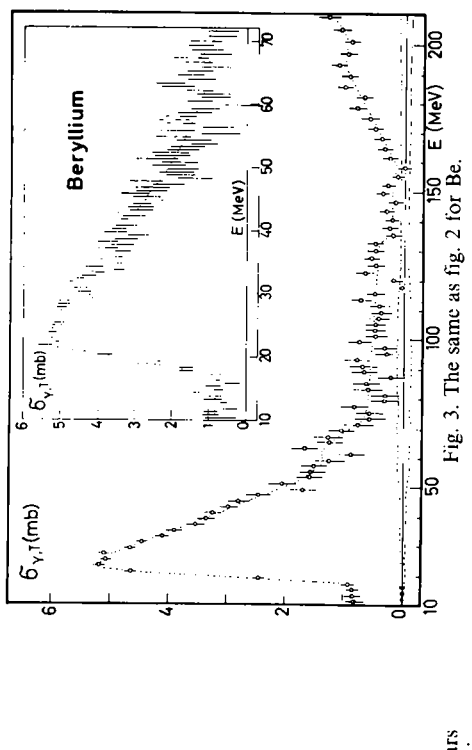

Fig. 3. The same as fig. 2 for Be.

Fig. 4. The same as fig. 2 for C.

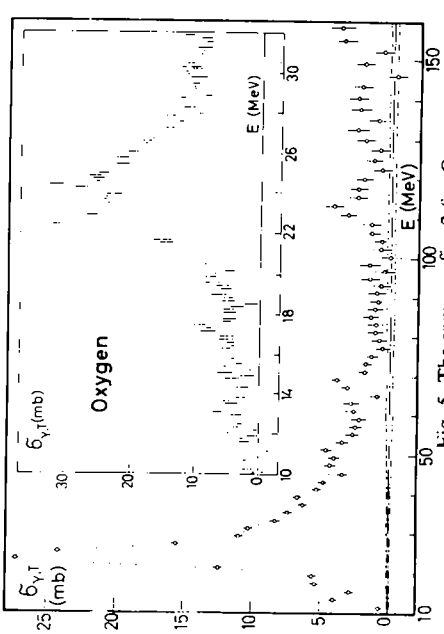

Fig. 5. The same as fig. 2 for O.

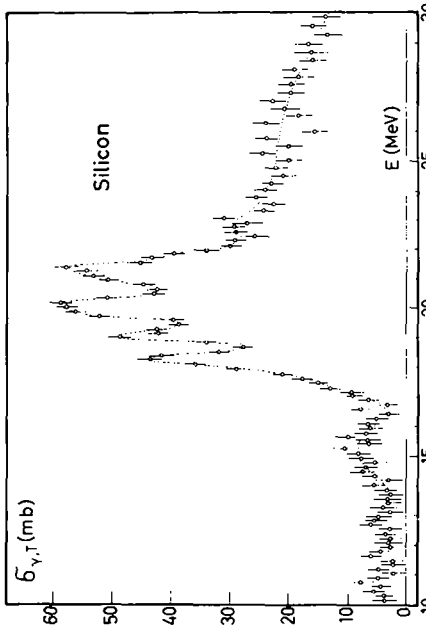

Fig. 7. Total photonuclear cross section for Si. Above 60 MeV the total attenuation cross section of Si displays a structure which can qualitatively be described by coherent pair production in the monocrystalline absorber rods (Überall effect)[11]). A more accurate measurement of this effect is in preparation. An unambiguous determination of the nuclear cross section above 50 MeV therefore turned out to be impossible.

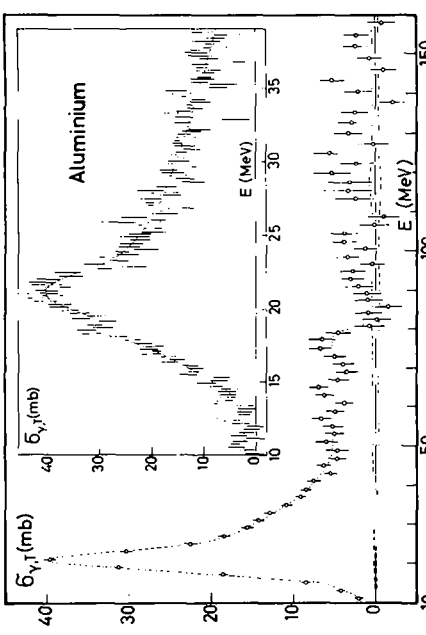

Fig. 6. The same as fig. 2 for Al.

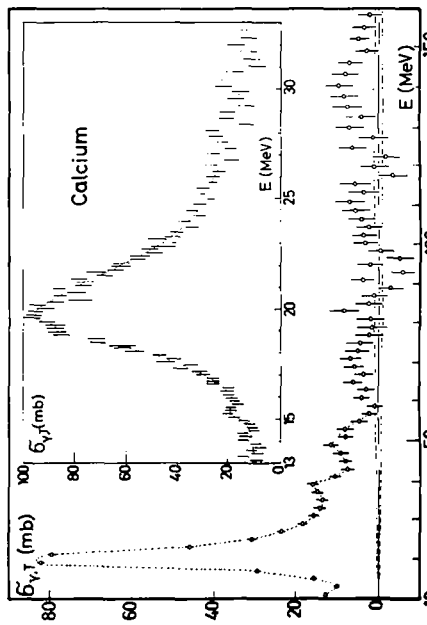

Fig. 8. The same as fig. 2 for Ca.

spectrometer. The period of these oscillations cannot be smaller than the energy span covered by one energy setting of the spectrometer, which amounts to 10% in photon energy.

(b) Systematic errors due to uncertainties in the attenuator properties are listed in table 1. These errors are associated with the determination of the number of nuclei per cm^2 in the absorber. For the graphite rods used a careful almost point-to-point density measurement had to be made because of density inhomogenities of the order of $\pm 1\%$.

(c) Systematic errors that arise from uncertainties in the correction for dead time losses in the counter systems of the spectrometers are given in the last column of table 1 ($\Delta\sigma_{\gamma,T}$ dead time (mb)).

(d) Systematic errors may arise from the non-ideal geometry of every actual attenuation experiment. The probability of detecting Compton scattered photons from the absorber by the main spectrometer can be calculated and was found to be negligible. The detection of secondary bremsstrahlung produced by pair electrons in an absorber of high Z (Pb) was checked by placing the absorber at different distances from the main spectrometer. No statistically significant influence on the measured cross sections was observed.

(e) An error on spectrometer energy calibration may influence the value of the resulting $\sigma_{\gamma,T}$, especially in those energy regions where the non-nuclear cross section σ_{el} is a rapidly varying function of the photon energy. The energy assigned to counter i for a spectrometer setting denoted by a nominal photon energy E' is given by the center of response energy E_i,

$$E_i = \frac{\int E A_i(E', E)\mathrm{d}E}{\int A_i(E', E)\mathrm{d}E},$$

where $A_i(E', E)$ is the response function [3]) of counter i. It can be shown that the use of E_i, instead of an unfolding technique, gives identical results for even the steepest part of actual cross sections at low energies. The uncertainties in the photon energy E_i assigned to the counter i for a given magnetic field were carefully examined and resulted in an error of $\Delta E/E = 0.1\%$. The influence of this uncertainty on the $\sigma_{\gamma,T}$ determination can be neglected.

(f) Energy fluctuations of the electrons passing the energy slits of the deflecting systems ($\Delta E/E = \pm 1\%$) and fluctuations of beam position or direction, produce an error which is random in character. Repeated measurements at the same energy showed fluctuations of the cross sections which were consistent with those expected from counting statistics alone. The influences of beam energy and geometry fluctuations were therefore neglected.

(g) Finally, and most importantly, the incomplete knowledge of the non-nuclear cross sections introduces systematic errors. A few corrections to an earlier compilation of these cross sections [6]) were applied. The non-nuclear cross sections used in this paper are:

(*i*) *Atomic photoeffect.* Negligible for the low-Z elements investigated here.

(*ii*) *Compton scattering.* Klein-Nishina formula with radiative corrections including double Compton effect.

(*iii*) *Pair production in the field of the nucleus.* Bethe-Heitler [7]) unscreened cross section with radiative correction [8]); screening corrections calculated using a method given by Sørensen [9]) with Hartree-Fock form factors up to 0.3 m_0c momentum transfer and a smoothly fitted Thomas-Fermi form factor from there on. The Coulomb correction has been determined experimentally by attenuation measurements of high-Z elements (Cu, Sn, Ta, Pb) assuming the nuclear cross section for these elements is either known (from (γ, n) experiments [10])) or negligible (above 50 MeV). Although this correction is important for high-Z elements, it is small for the elements investigated here because of its Z^4 dependence. The lack of reliable theoretical calculations for the Coulomb correction between 10 and 50 MeV certainly restricts the range in Z available for absolute $\sigma_{\gamma,\mathrm{T}}$ measurements to $Z \leqq 20$.

(*iv*) *Pair production in the field of the electron (triplet production).* Borsellino-Ghizzetti's formula corrected for screening and radiation effects [6]).

In summary, we estimate the error of the sum of all non-nuclear cross sections (*i*)–(*iv*) to be smaller than 0.1 % for the elements and the energy range considered here.

4. Experimental results

4.1. CROSS SECTIONS

The total nuclear photon absorption cross sections obtained in the present series of experiments are shown in figs. 2 to 8. The plotted values are statistically weighted averages of the measured cross sections in the given energy bins. Except for the cross sections of carbon, no normalization to the calculated non-nuclear cross sections has been made. In the case of carbon the measured total attenuation cross sections $\sigma_{\mathrm{tot}}(E)$ have been increased by 0.15 % in order to match the cross section to zero at 10 MeV. This increase is smaller than the systematic error which arises from uncertainties in the determination of the density of the carbon absorber. The lengths of the error bars given in figs. 2 to 8 are determined by the counting statistics of the main spectrometer, and the dashed lines along the abscissa indicate the magnitude of possible oscillations produced by the counting statistics of the normalizing spectrometer [see subsect. 3(a)]. The dotted and dashed lines through the cross section values have been drawn to guide the eye.

For all elements the cross sections in the region of the giant resonance agree well with other experimental results [2]). No unfolding procedure has been applied to obtain the structures in the cross sections of C, O, and Si (10 to 30 MeV). Measurements with improved resolution (0.7 % instead of 1.1 %) did not result in statistically significant changes of these structures. All measured cross sections have therefore been used to obtain the averaged values shown.

4.2. MOMENTS AND MEAN ENERGIES

The predictions of the sum rules concern in general the values of the moments $\sum_\alpha(0, \hat{E})$ of the cross section $\sigma_{\gamma,T}(E)$. These moments are defined by

$$\sum_\alpha(0, \hat{E}) = \int_0^{\hat{E}} E^\alpha \sigma_{\gamma,T}(E) \mathrm{d}E. \tag{1}$$

TABLE 2

The moments of the experimental nuclear cross section distributions integrated from 10 MeV to the energy $\hat{E}$, and their statistical errors

	$\hat{E}$ (MeV)	$\sum_{-2}$ (mb/MeV)	±(%)	$\sum_{-1}$ (mb)	±(%)	$\sum_0$ (mb·MeV)	±(%)	$\sum_{+1}$ (b·MeV^2)	±(%)	$\sum_{+2}$ (b·MeV^3)	±(%)
Li	100	0.196	1.1	4.64	1.0	143	1.7	5.82	3.1	305	5
	140	0.197	1.1	4.79	1.0	161	1.9	8.03	3.4	577	5
	210	0.198	1.1	5.03	1.0	206	2.0	16.60	3.7	2220	5
Be	100	0.192	2.5	5.19	1.5	173	2.0	7.11	3.4	362	5
	140	0.194	2.5	5.33	1.5	189	2.1	9.09	3.6	600	6
	210	0.195	2.5	5.58	1.5	236	2.1	17.80	3.5	2240	5
C	100	0.313	1.7	8.81	1.1	291	1.6	12.00	2.9	630	4
	140	0.316	1.7	9.18	1.2	334	2.2	17.10	5	1250	7
O	100	0.580	1.6	14.50	1.3	432	2.0	16.00	4	748	8
	140	0.585	1.6	15.10	1.3	508	2.5	25.20	5	1880	8
Al	100	1.10	1.8	25.70	1.5	739	2.6	27.9	5	1400	8
	140	1.11	1.8	26.3	1.7	807	3.9	36.4	9	2450	16
Ca	100	2.22	1.2	45.5	1.5	1120	3.6	34.9	9	1430	18
	140	2.23	1.2	46.8	1.7	1290	4.6	56.6	11	3710	19

From the cross sections given above only the contributions to this integral from 10 MeV up to $\hat{E}$, $\sum_\alpha(10, \hat{E})$, can be obtained. The values of these contributions are different from the moments defined in eq. (1) if a particle emission threshold lies below 10 MeV and if this results in an appreciable contribution $\sum_\alpha(0, 10)$ to the moments below 10 MeV. This is the case for Li [ref. [12])] and Be [ref. [13])] especially for $\alpha = -1$ and -2. The experimental values of the moments are given for $\alpha = 0, \pm 1$ and ± 2 in table 2. The errors of these values also given in table 2 have been calculated using counting statistics alone.

5. Discussion

There is no theory which predicts total photonuclear cross sections in the whole energy range covered by this experiment. Usually this entire range is subdivided into two regions called the "giant dipole resonance region" and the region "above the giant dipole resonance" or "at intermediate energies". Theories have been developed

that describe just one of the two regions. The photon energy at which the two regions meet is roughly the energy where results from shell model calculations describing the giant dipole resonance region fall off too rapidly with increasing energy compared to experiment and where theories for the intermediate energies are not yet valid. This most uncertain photon energy region can be considered as located around 40 MeV. Experimentally (see figs. 2 to 8) one certainly cannot identify a special feature of the cross sections in this energy region (30 to 40 MeV) which would reflect the transition from one theoretical description to an other.

In the following subsections cross sections from theories valid in either of the two regions mentioned above are compared with the experimental results. Furthermore model-independent predictions for the moments of the summed oscillator strength of all particles in the nucleus (sum rules) are discussed.

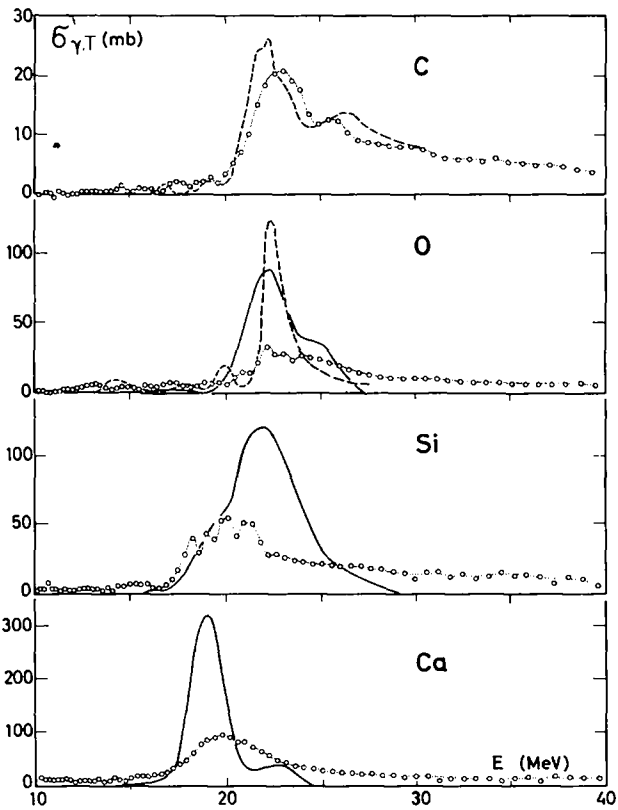

Fig. 9. Comparison between experiment and theory in the giant resonance region. Open circles and dotted line: experiment; dashed line for carbon: ref. [14]); dashed line for oxygen: ref. [15]); full lines: ref. [16]).

5.1. THE GIANT RESONANCE REGION

The most recent predictions of total photonuclear cross sections [14-16]) in the giant resonance region are compared with the experimental values in fig. 9. Except for one

case (carbon) there is a disagreement in the magnitude of the cross sections between experiment and theory by a factor of 3 to 4. Since experimental errors certainly cannot account for the discrepancy, approximations used in the theories must be responsible. The most important approximation is the restriction to 1p-1h excitations and the limitation in the number of outgoing channels. The good agreement between experimental and theoretical results for carbon was achieved by a calculation [14]) taking into account all intermediate coupling shell model states of the residual mass-11 nuclei below 10 MeV excitation energy (26 outgoing channels).

5.2. THE INTERMEDIATE ENERGY REGION

The first attempt to describe the region above the giant resonance was published by Levinger [17]). His prediction for the total photonuclear cross section was

$$\sigma_L(E) = 8\frac{NZ}{A}\sigma_D(E) = 300\frac{NZ}{A}(E-B)^{\frac{3}{2}}E^{-3} \qquad \text{(mb)}. \tag{2}$$

In this expression the energy dependence is given by the deuteron photodisintegration cross section $\sigma_D(E)$ for which the Bethe-Peierls formula has been inserted. The binding energy B of the free deuteron and the photon energy E have to be inserted in units of MeV. For the elements Li, Be, C and O this quasideuteron formula compares well with the energy dependence and the absolute magnitude of the cross sections measured in the energy region from 40 to 100 MeV. Below 30 MeV no similarity between experiment and the quasideuteron theory can be expected. The density of the deuteron-like structures in the nucleus is the only parameter in formula (2) which sometimes is subject to refined calculations [18]). The results given above agree with Levinger's original value of 8 NZ/A. This agreement indicates that the absorption mechanism above 40 MeV is dominated by the absorption of photons by correlated pairs of particles which results in a (γ, np) reaction; this is consistent with the large ratio of total cross section to single-particle cross section found experimentally in this energy region. With Cook's [19]) values for $\sigma_{\gamma,n}$ the ratio $\sigma_{\gamma,T}/\sigma_{\gamma,n}$ is approximately 5 in the energy range, where σ_L describes the experimental results for C and O.

There were several attempts to go beyond shell model calculations by introducing nucleon-nucleon correlations [20]), but these calculations were not able to give a satisfactory description of photonuclear reactions.

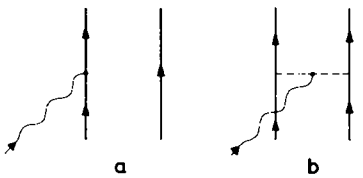

Fig. 10. (a) Photon interaction in the pure shell model. (b) Typical exchange contribution, giving rise to the (γ, np) effect and an enhancement of the integrated cross section $\sum_0$ over the classical sum.

Recently, Gari and Hebach [21]) developed a model for photonuclear reactions at intermediate energies (above 50 MeV), which introduces the nucleon-nucleon correlations in a consistent way ensuring orthogonality and gauge invariance.

In this model not only the graphs of the type given in fig. 10a are taken into account but also graphs of the type given in fig. 10b. Up to now only ^{4}He reactions have been calculated with this model. Qualitatively the results agree with the conclusions derived from Levinger's quasi-deuteron model concerning the dominance of the (γ, np) reaction. It appears very desirable to obtain quantitative theoretical results from this model for the elements investigated experimentally in this paper.

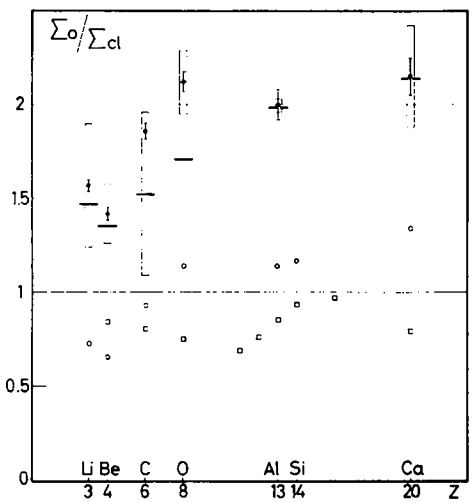

Fig. 11. Integrated cross sections $\sum_0(10, \hat{E})$ for $\hat{E} = 35$ MeV (open circles) and for $\hat{E} = 140$ MeV (closed circles) in units of the classical sum $\sum_{cl}$. For comparison, the integrated cross sections for $\hat{E} = 35$ MeV from ref. [3]) are plotted (open squares). The error bars at the values for $\hat{E} = 140$ MeV indicate one standard deviation from counting statistics in the spectrometers. The rectangles give the maximum and minimum possible values that the integrated cross sections may have from uncertainties in absorber characteristics. Despite this uncertainty and the uncertainty of roughly 0.1 % in the non-nuclear cross sections, a lower limit for the $\sum_0$ values can be given (short solid line), which follows from the simple requirement that nuclear cross sections cannot be negative (no interference between nuclear and non-nuclear effects). The contribution $\sum_0(0, 10)$ for the integrated cross section of ^{9}Be is 0.06 ± 0.005 $\sum_{cl}$ [ref. [13])].

5.3. SUM RULES AND RELATED NUMBERS

The integrated cross sections $\sum_0(10, \hat{E})$ expressed in units of the classical dipole sum $\sum_{cl} = 60\,NZ/A$ (mb · MeV) for $\hat{E} = 35$ MeV and $\hat{E} = 140$ MeV are shown in fig. 11 where they are compared with the NBS values [22]) for $\hat{E} = 35$ MeV. The values for $\hat{E} = 140$ MeV exceed those for $\hat{E} = 35$ MeV by roughly a factor of 2. These results agree with the integrated cross section $\sum_0(10, 80) = 1.4$ obtained in an earlier photon scattering experiment [23]) with an upper energy limit of 80 MeV. From this agreement the assumptions leading to the integrated cross section value 1.4 from the photon scattering data seem to be justified. The most important of

these assumptions is the dominance of elastic photon scattering over inelastic processes. Levinger [1]) predicted a value of $\sum_0$ larger than $\sum_{cl}$ for the case where the nucleonic interaction is mediated by charged pions. Naively one can think of the extra charge provided in such an exchange process (fig. 10b) as causing an increased absorption.

Levinger [1]) and Migdal [24]) have defined mean energies

$$E_\alpha(\hat{E}) = \frac{\sum_\alpha(0, \hat{E})}{\sum_{\alpha-1}(0, \hat{E})}, \tag{3}$$

and

$$E_M(\hat{E}) = \sqrt{\frac{\sum_0(0, \hat{E})}{\sum_{-\alpha}(0, \hat{E})}},$$

respectively, and, from general, model independent considerations, Levinger has shown that the inequality

$$E_\alpha(\hat{E}) \geq E_{\alpha-1}(\hat{E}) \tag{4}$$

must hold, furthermore, that the Migdal energy $E_M(\hat{E})$ should fall between $E_0(\hat{E})$ and $E_{-1}(\hat{E})$. In table 3 these mean energies are presented in the form of the ratios

$$r_\alpha = \frac{E_\alpha}{E_{\alpha-1}} = \frac{\sum_\alpha \sum_{\alpha-2}}{\sum^2_{\alpha-1}}$$

for $\alpha = 0, +1$ and $+2$ and for $\hat{E} = 100$ MeV and $\hat{E} = 140$ MeV. The ratio E_M/E_{-1} and the quantity $A^{\frac{1}{3}}E_M$ are also given in table 3.

TABLE 3

The experimental values for the three ratios of mean energies $r_\alpha = \sum_{\alpha-2}\sum_\alpha/\sum^2_{\alpha-1}$, the Migdal energy $E_M A^{\frac{1}{3}}$ and the ratio E_M/E_{-1}

	$\hat{E}$ (MeV)	r_{+2}	r_{+1}	r_0	$E_M A^{\frac{1}{3}}$ (MeV)	E_M/E_{-1}
Li	100	1.29	1.32	1.31	52	1.14
	140	1.44	1.48	1.38	55	1.18
	210	1.66	1.97	1.61	62	1.27
Be	100	1.24	1.23	1.23	62	1.11
	140	1.37	1.36	1.29	65	1.14
	210	1.67	1.78	1.48	72	1.22
C	100	1.27	1.25	1.17	70	1.08
	140	1.43	1.41	1.25	74	1.12
O	100	1.26	1.24	1.19	69	1.09
	140	1.50	1.47	1.30	74	1.14
Al	100	1.33	1.31	1.23	78	1.11
	140	1.49	1.47	1.29	81	1.14
Ca	100	1.31	1.27	1.20	77	1.10
	140	1.49	1.59	1.31	82	1.15

From the experimental values of table 3, it can be seen that the inequality of eq. (4) is true, and that the Migdal energy indeed lies between $E_0(\hat{E})$ and $E_{-1}(\hat{E})$. It is perhaps also significant that the values of the ratios r_α are similar to each other for $\alpha = 0, +1$ and $+2$ and vary only slowly with Z.

Since $\sum_{-1}$ and $\sum_{+1}$ are measures for the ground state mean square radius $\langle r^2 \rangle_{00}$ and mean square momentum $\langle p^2 \rangle_{00}$ the ratio $r_1 = \sum_{-1} \sum_{+1} / \sum_0^2$ reflects the uncertainty principle. The numerical value of r_1 therefore should depend only on the shape of the potential in which the nucleons move. From this experiment we obtain $r_1 = 1.46 \pm 0.08$.

References

1) J. S. Levinger, Nuclear photo-disintegration (Oxford Univ. Press, 1960)
2) B. Ziegler, Nucl. Phys. **17** (1960) 238;
   B. S. Dolbilkin and F. A. Nikolaev, Proc. P. N. Lebedev Phys. Inst. **36** (1967);
   N. Bezić, D. Brajnik, D. Jamnik and G. Kernel, Nucl. Phys. **A128** (1969) 426;
   J. M. Wyckoff, B. Ziegler, H. W. Koch and R. Uhlig, Phys. Rev. **137** (1965) B576
3) J. Ahrens, H. Borchert, A. Zieger and B. Ziegler, Nucl. Instr. **108** (1973) 517
4) H. Ehrenberg *et al.*, Nucl. Instr. **105** (1972) 253
5) J. Ahrens *et al.*, Proc. Int. Conf. on nuclear structure studies using electron scattering and photoreaction, Sendai, 1972 (Research Report of Lab. of Nuclear Science, Tohoku Univ., vol. 5, 1972) p. 213
6) J. H. Hubbell, Photon cross sections, attenuation coefficients and energy absorption coefficients from 10 keV to 100 GeV (NSRDS-NBS 29, US Government Printing Office, Washington, 1969)
7) H. Bethe and W. Heitler, Proc. Roy. Soc. **A146** (1934) 83
8) K. Mork and H. Olsen, Phys. Rev. **140** (1965) B1661
9) A. Sørenssen, Nuovo Cim. **38** (1965) 745; **41A** (1966) 543
10) S. C. Fultz, R. L. Bramblett, J. T. Caldwell and R. R. Harvey, Phys. Rev. **133** (1964) B1149;
    S. C. Fultz, B. L. Berman, J. T. Caldwell, R. L. Bramblett and M. A. Kelly, Phys. Rev. **186** (1969) 1255;
    R. Bergère, H. Beil and A. Veyssière, Nucl. Phys. **A121** (1968) 463;
    A. Veyssière, H. Beil, R. Bergère, P. Carlos and A. Leprêtre, Nucl. Phys. **A159** (1970) 561;
    R. R. Harvey, J. T. Caldwell, R. L. Bramblett and S. C. Fultz, Phys. Rev. **136** (1964) B126
11) H. Überall, Phys. Rev. **103** (1956) 1055;
    G. Diambrini Palazzi, Rev. Mod. Phys. **40** (1968) 611
12) R. L. Bramblett, B. L. Berman, M. A. Kelly, J. T. Caldwell and S. C. Fultz, Proc. Int. Conf. on photonuclear reactions and applications, Asilomar, 1973 (National Technical Information Service US Department of Commerce, Springfield, Va) p. 175
13) R. J. Hughes, R. H. Sambell, E. G. Muirhead and B. M. Spicer, Nucl. Phys. **A238** (1975) 189
14) J. Birkholz, Phys. Lett. **34B** (1971) 1
15) S. Krewald, J. Birkholz, A. Faessler and J. Speth, Proc. Int. Conf. on nuclear structure and spectroscopy, Amsterdam, 1974, vol. 2 (Scholar's Press, Amsterdam) p. 111
16) S. S. M. Wong, D. J. Rowe and J. C. Parikh, Phys. Lett. **48B** (1974) 403
17) J. S. Levinger, Phys. Rev. **84** (1951) 43
18) H. Schier and B. Schoch, Nucl. Phys. **A229** (1974) 93
19) B. C. Cook, J. E. E. Baglin, J. N. Bradford and J. E. Griffin, Phys. Rev. **143** (1966) 724, 712
20) M. Fink, H. Hebach and H. Kümmel, Nucl. Phys. **A186** (1972) 353;
    W. Weise and M. G. Huber, Nucl. Phys. **A162** (1971) 330;
    G. M. Shklyarevskii, JETP (Sov. Phys.) **14** (1962) 324;
    A. Malecki and P. Picchi, Nuovo Cim. Lett. **8** (1973) 16
21) M. Gari and H. Hebach, Phys. Rev. **C10** (1974) 1629
22) E. G. Fuller, Proc. Int. Conf. on photonuclear reactions and Applications, Asilomar, 1973 (National Technical Information Service US Department of Commerce, Springfield, Va) 1201
23) J. Ahrens, H. Borchert, K.-H. Czock, D. Mehlig and B. Ziegler, Phys. Lett. **31B** (1970) 570
24) A. Migdal, J. Phys. USSR **8** (1944) 331